

Perturbative QCD Calculations of Elliptic Flow and Shear Viscosity in Au+Au Collisions at $\sqrt{s_{NN}} = 200$ GeV

Zhe Xu,¹ Carsten Greiner,¹ and Horst Stöcker²

¹*Institut für Theoretische Physik, Goethe-Universität Frankfurt, Max-von-Laue-Strasse 1, D-60438 Frankfurt am Main, Germany*

²*Gesellschaft für Schwerionenforschung mbH (GSI), Planckstrasse 1, D-64291 Darmstadt, Germany*
(Dated: October 26, 2018)

The elliptic flow v_2 and the ratio of the shear viscosity over the entropy density, η/s , of gluon matter are calculated from the perturbative QCD (pQCD) based parton cascade Boltzmann approach of multiparton scatterings. For Au+Au collisions at $\sqrt{s} = 200$ A GeV the gluon plasma generates large v_2 values measured at the BNL Relativistic Heavy Ion Collider. Standard pQCD yields $\eta/s \approx 0.08 - 0.15$ as small as the lower bound found from the anti-de Sitter/conformal field theory conjecture.

PACS numbers: 25.75.Ld, 12.38.Mh, 24.10.Lx, 51.20.+d

The large values of the elliptic flow v_2 measured at the Relativistic Heavy Ion Collider (RHIC) [1] indicate that the matter created, the quark gluon plasma (QGP), behaves as a nearly perfect fluid exhibiting strong “explosive” collective motion. As transport coefficients like the shear viscosity characterize the dynamics of the QGP [2], it is obvious that a less viscous medium will generate larger v_2 values. Now, ideal hydrodynamical calculations have reproduced the observed v_2 dependence on centrality (within 30%), mass, and transverse momentum p_T (for $p_T < 1.5$ GeV) [3]. Hence, the QGP created possesses a small viscosity coefficient [4]. The smallness of the viscosity is of great interest as a result of the recent debate about speculative “realizations” of supersymmetric representations of Yang-Mills theories using the anti-de Sitter/conformal field theory (AdS/CFT) conjecture [5]. On the other hand, calculations done within ideal hydrodynamics failed to reproduce the v_2 at higher centrality, at higher transverse momentum, and its dependence on rapidity [6]. Although recent calculation within viscous hydrodynamics [7] can fit the centrality dependence of v_2 , the p_T dependence cannot be obtained consistently. One drawback in these calculations is the assumed ideal thermal initial conditions. In principle, the entire process of the nuclear collision is theoretically better studied by using a consistent microscopic transport theory. Transport simulations can provide the correct viscous hydrodynamics when the system is near equilibrium. Moreover, nonequilibrium processes, like equilibration and the onset and the breakdown of viscous hydrodynamics, are involved. However, both hadronic [8] and partonic [9] cascade calculations with $2 \rightarrow 2$ processes failed to yield the large v_2 values observed at RHIC.

Recently we have developed a relativistic perturbative QCD (pQCD) based on-shell parton cascade Boltzmann approach of multiparton scatterings (BAMPS) [10, 11] to study, on a semiclassical level, the dynamics of gluon matter produced in Au+Au collisions at RHIC energies. Although coherent quantum effects like color instabili-

ties [12] may play a role at the very initial stage where the matter is superdense, it is the pQCD interaction that drives the gluon matter to equilibrium within a time interval of 1 fm/c. The fast thermalization observed is due to gluon bremsstrahlung [11]. This process is also responsible for the small ratio of the shear viscosity to the entropy density, η/s , for a static gluon gas [13]. For a coupling constant $\alpha_s = 0.6(0.3)$ we obtain $\eta/s = 0.076(0.13)$, which is as small as the lower bound $\eta/s = 1/4\pi$ found from the AdS/CFT conjecture [5]. Hence, pQCD interactions can explain why the QGP created at RHIC is strongly coupled and behaves like a nearly perfect fluid. There is no need to invoke exotic black hole physics in higher dimensions and supersymmetric Yang-Mills theories using the AdS/CFT conjecture to understand RHIC data.

In this Letter we employ BAMPS to calculate the elliptic flow v_2 of gluons in Au+Au collisions at $\sqrt{s} = 200$ A GeV. For a firm footing we compare our results with the experimental data, assuming parton-hadron duality. To see how viscous the gluon plasma behaves, the ratio of shear viscosity to entropy density is calculated.

The initial gluon distributions are taken as given in Ref. [11]: an ensemble of minijets with transverse momenta greater than 1.4 GeV, produced via semihard nucleon-nucleon collisions. We use Glauber geometry with a Woods-Saxon profile and assume independent binary nucleon-nucleon collisions. A formation time for initial minijets is also included [10, 11]. In contrast to the Glauber-type initial condition, the color-glass-condensate-type initial condition provides larger initial eccentricity and thus might yield larger v_2 values [14]. Including quarks in BAMPS is in progress. We do not expect large changes in the present results shown below, because the quark amount at RHIC is initially only 20%. As quarks are less interactive than gluons, the total v_2 will be slightly smaller than that obtained in a pure gluon matter.

Gluon interactions included in BAMPS are

elastic scatterings with the pQCD cross section $d\sigma^{gg \rightarrow gg}/dq_{\perp}^2 = 9\pi\alpha_s^2/(q_{\perp}^2 + m_D^2)^2$, as well as pQCD inspired bremsstrahlung $gg \leftrightarrow ggg$ with the effective matrix element [15]

$$|\mathcal{M}_{gg \rightarrow ggg}|^2 = \frac{9g^4}{2} \frac{s^2}{(\mathbf{q}_{\perp}^2 + m_D^2)^2} \frac{12g^2\mathbf{q}_{\perp}^2}{\mathbf{k}_{\perp}^2[(\mathbf{k}_{\perp} - \mathbf{q}_{\perp})^2 + m_D^2]} \Theta(k_{\perp}\Lambda_g - \cosh y), \quad (1)$$

where $g^2 = 4\pi\alpha_s$. \mathbf{q}_{\perp} and \mathbf{k}_{\perp} denote the perpendicular component of the momentum transfer and of the radiated gluon momentum in the center-of-mass frame of the collision, respectively. y is the momentum rapidity of the radiated gluon in the center-of-mass frame, and Λ_g is the gluon mean free path, which is calculated self-consistently [10]. The interactions of the massless gluons are screened by a Debye mass $m_D^2 = \pi d_G \alpha_s N_c \int d^3p/(2\pi)^3 \cdot f/p$, where $d_G = 16$ is the gluon degeneracy factor for $N_c = 3$. m_D is calculated locally using the gluon density function f obtained from the BAMPS simulation. The suppression of the bremsstrahlung due to the Landau-Pomeranchuk-Migdal effect is taken into account within the Bethe-Heitler regime using the step function in Eq. (1).

In the present pQCD simulations the interactions of the gluons are stopped when the local energy density drops below 1 GeV/fm³. This value is assumed to be the critical value for the occurrence of hadronization, below which parton dynamics is not valid. Because hadronization and hadronic cascade are not yet included in BAMPS, a gluon, which ceases to interact, propagates freely and can be regarded as a free pion according to the parton-hadron duality.

In Table I the initial and final transverse energy per rapidity $dE_T/dy(|y| < 1.5)$ for 6 centrality bins are listed, which are obtained from BAMPS using two different coupling constants.

The PHOBOS values are extracted from the p_T spectra for charged hadrons [16], i.e., $dE_T = \int dp_T \sqrt{p_T^2 + m_0^2} \times dN/dp_T$ with m_0 being the pion mass. To compare with them we have multiplied a factor of 2/3 to dE_T/dy for gluons. The dE_T/dy using $\alpha_s = 0.3(0.6)$ is slightly larger(smaller) than the PHOBOS data within $\pm 8\%$.

TABLE I: Centrality dependence of the transverse energy per rapidity at midrapidity. Dimension is GeV.

Centrality	PHOBOS	Initial	Final $\alpha_s = 0.3$	Final $\alpha_s = 0.6$
45%-50%	58	85	61	55
35%-45%	85	132	89	80
25%-35%	132	220	138	122
15%-25%	198	354	209	182
6%-15%	281	535	299	257
0%-6%	368	707	380	324

Figure 1 shows the rapidity dependence of the initial and final dE_T/dy (solid curves with open symbols) for the most central 5% collisions, compared with the BRAHMS data for the charged meson rapidity distributions, $dE_T/dy = m_T dN/dy$ [17]. The shape of dE_T/dy obtained from BAMPS agrees well with the BRAHMS data within $y < 2.5$.

The chosen initial condition of minijets, with $p_0 = 1.4$ GeV as a parameter, seems appropriate for describing the experimental data. However, calculations with the same initial condition and employing only elastic pQCD $gg \rightarrow gg$ interactions show much less decrease of dE_T/dy [10] (see dashed curves with solid symbols in Fig. 1).

Figure 2 shows the elliptic flow v_2 at midrapidity and its dependence on rapidity, as obtained from the BAMPS calculations with $\alpha_s = 0.3$, and 0.6. These are compared with the PHOBOS data [18].

Except for the central centrality region the results with $\alpha_s = 0.6$ agree perfectly with the experimental data, whereas the results with $\alpha_s = 0.3$ are roughly 20% smaller. The results with only $gg \rightarrow gg$ interactions (dashed curves with solid symbols) are much smaller than the data, which demonstrates that bremsstrahlung and backreactions are the dominant processes in generating large elliptic flow.

Figure 3 shows the generation of the elliptic flow at midrapidity for noncentral Au+Au collisions with impact parameter $b = 8.6$ fm corresponding to $\langle N_{\text{part}} \rangle = 111$.

v_2 increases strongly during the early stage of thermal equilibration (time scale $\lesssim 1$ fm/c) where hydrodynamics is not valid but where the eccentricity is largest. The generation rate of v_2 during thermalization is only slightly smaller than that during the subsequent (viscous) hydrodynamical expansion. The v_2 generation ends at 3 fm/c, where the critical energy density is reached for all the gluons at midrapidity.

Hence, the generation of the large elliptic flow observed

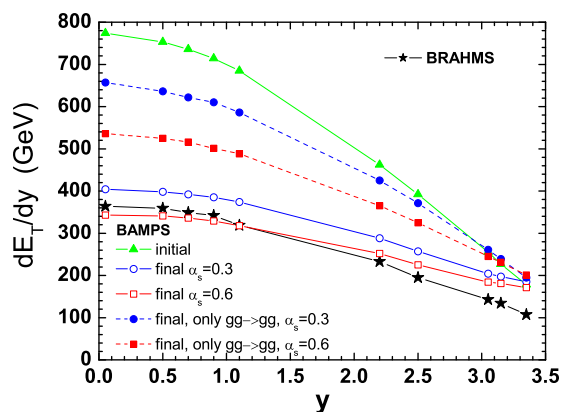


FIG. 1: (color online). Rapidity dependence of the transverse energy per rapidity. Results from BAMPS are multiplied by a factor of 2/3 to compare with the BRAHMS data for charged mesons.

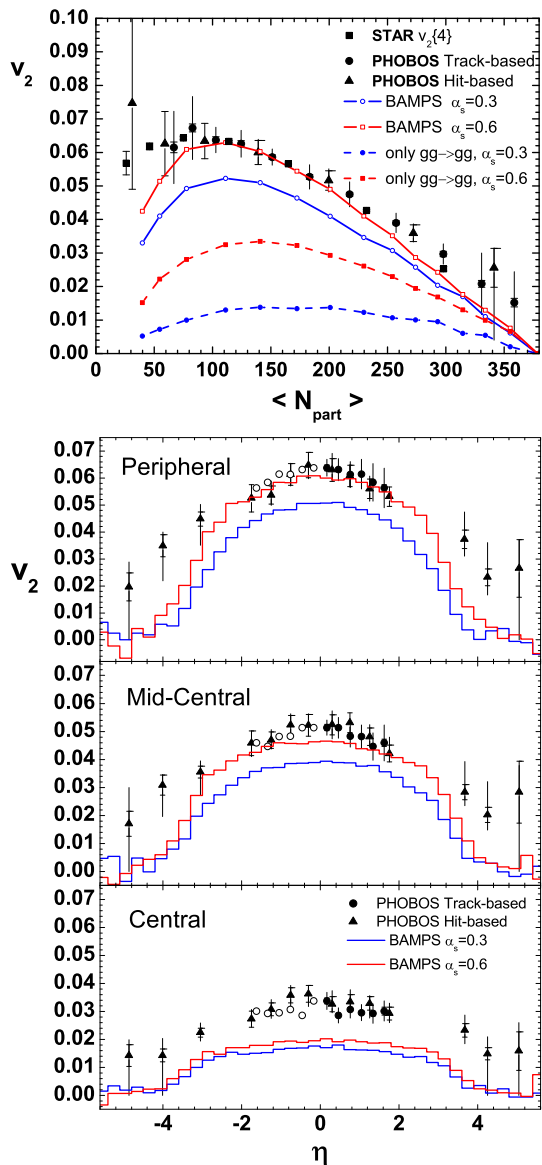


FIG. 2: (color online). Upper panel: Elliptic flow $v_2(|y| < 1)$ from BAMPS using $\alpha_s = 0.3$ and 0.6 , compared with the RHIC data [18]. Lower panels: Pseudorapidity dependence of elliptic flow for three centrality classes ranging from peripheral to central (25% – 50%, 15% – 25%, and 0% – 15%) from top to bottom.

at RHIC is well described by pure perturbative gluon interactions as incorporated in BAMPS. It is consistent with the decrease of the transverse energy due to the mechanical work done by the pressure during the expansion. Inclusion of hadronization [19] and subsequent hadronic cascade [20] will yield only moderate contributions to the final elliptic flow values, as the densities are already rather low and the eccentricity becomes small.

The ratio of the shear viscosity to the entropy density, η/s , is extracted from the BAMPS calculations (including $gg \leftrightarrow ggg$) to see how viscous the gluon matter is for generating the large v_2 values that match the experimen-

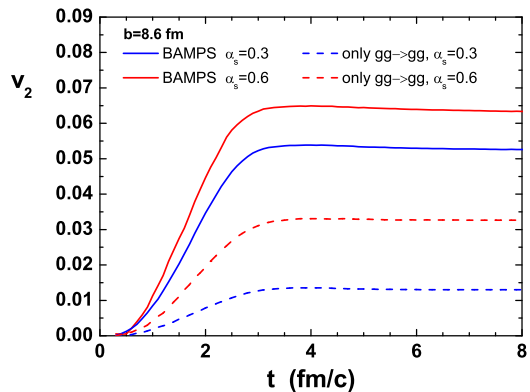


FIG. 3: (color online). Generation of elliptic flow at midrapidity for a noncentral collision with an impact parameter of $b = 8.6$ fm.

tal data. We obtain the shear viscosity as [13]

$$\eta \cong \frac{1}{5} n \frac{\langle E(\frac{1}{3} - v_z^2) \rangle}{\frac{1}{3} - \langle v_z^2 \rangle} \frac{1}{\sum R^{\text{tr}} + \frac{3}{2} R_{23} - R_{32}}, \quad (2)$$

where n is the gluon density, E is the gluon energy, and $v_z = p_z/E$ is the velocity in the beam direction. $\sum R^{\text{tr}}$ denotes the total transport collision rate [11] describing momentum isotropization. R_{23} and R_{32} are interaction rates for $gg \rightarrow ggg$ and its backreaction, respectively. The entropy density is extracted by assuming that the gluon matter is in local kinetic equilibrium, which gives $s = 4n - n \ln \lambda$, where $\lambda = n/n_{\text{eq}}$ defines the gluon fugacity. The true entropy density is expected to be (slightly) smaller, because overall kinetic equilibration cannot be complete in an expanding system.

Figure 4 depicts the shear viscosity over entropy density ratio η/s extracted locally at the central region during the entire expansion before decoupling.

The central region is the region with transverse radius of 1.5 fm and within the space-time rapidity interval $|\eta_t| < 0.2$, where $\eta_t = \frac{1}{2} \ln[(t+z)/(t-z)]$. The curves in

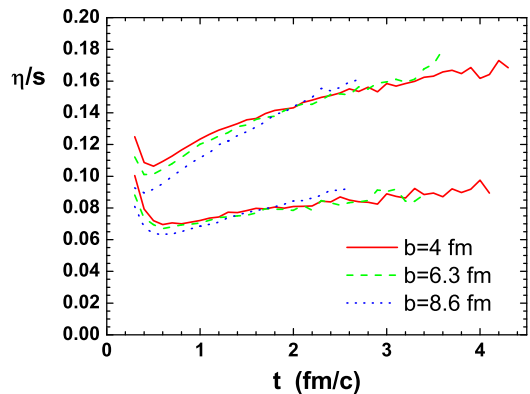


FIG. 4: (color online). Shear viscosity to entropy density ratio η/s at the central region. The upper band shows the results with $\alpha_s = 0.3$ and the lower band the results with $\alpha_s = 0.6$.

Fig.4 are obtained from BAMPS simulations with impact parameter $b = 4, 6.3, \text{ and } 8.6 \text{ fm}$, for $\alpha_s = 0.3 \text{ and } 0.6$. Note that during thermal equilibration (time scale $\lesssim 1 \text{ fm/c}$) Eq. (2) for calculating the shear viscosity is not fully valid and the true entropy density will be smaller than that given by the formula used.

The η/s ratio obtained from the simulations with the same α_s and for various impact parameters are almost the same, although the gluon density with $b = 8.6 \text{ fm}$ is significantly smaller than that with $b = 4 \text{ fm}$. Interaction rates and transport collision rates scale with the temperature T . The gluon fugacity is close to 1. Hence, η/s depends practically only on α_s . This also explains that the η/s values extracted in the outer transverse regions (not shown) are nearly the same as the ratio in the center. Figure 4 shows $\eta/s \approx 0.15$ for $\alpha_s = 0.3$ and $\eta/s \approx 0.08$ for $\alpha_s = 0.6$. These values agree well with those found for a static thermal gluon gas [13].

Figure 5 shows the cross sections of $gg \rightarrow gg$ and $gg \rightarrow ggg$ processes, extracted in the central region.

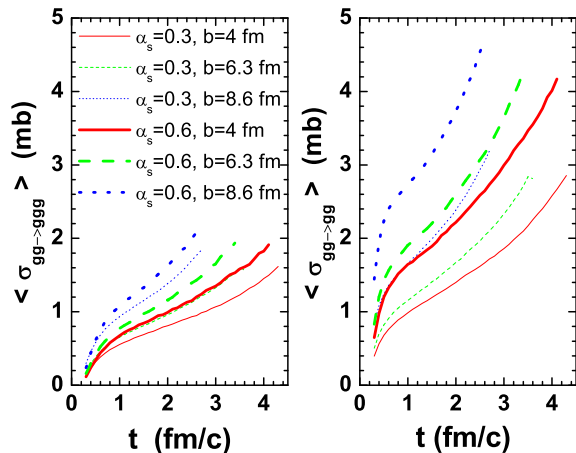


FIG. 5: (color online). Cross sections of $gg \rightarrow gg$ and $gg \rightarrow ggg$ processes in the central region.

Indeed, the cross section becomes larger when the density is smaller, so that $\langle \sigma \rangle T^2$ depends practically only on α_s . Note that the cross sections are indeed small. This demonstrates that it is not necessary to use unphysically large cross sections [9] or ultrashort hadronization times [8] to yield large v_2 values.

The pQCD based parton cascade BAMPS is used to calculate the elliptic flow v_2 and to extract the ratio of the shear viscosity to the entropy density, η/s , from simulations of Au+Au collisions at RHIC energy $\sqrt{s} = 200 \text{ A GeV}$. Simple parton-hadron duality allows one to compare our final v_2 results with the data measured at RHIC. Agreement between the data and theory is found with Glauber-type minijets initial conditions for gluons and with $\alpha_s = 0.3 - 0.6$. The η/s ratio of the gluon plasma created varies between 0.15 and 0.08. Standard pQCD interactions alone can describe the generation of large v_2 values at RHIC. The small η/s ratios found in the simula-

tions indicate that the gluon plasma created behaves like a nearly perfect fluid. This can be understood by perturbative QCD without resorting to exotic explanations such as the AdS/CFT conjecture: Gluon bremsstrahlung dominates and yields rapid thermalization, and therefore early pressure buildup and a small shear viscosity in the gluon gas.

The authors thank G. Burau and M. Gyulassy for fruitful discussions.

-
- [1] S. S. Adler *et al.* (PHENIX Collaboration), Phys. Rev. Lett. **91**, 182301 (2003); J. Adams *et al.* (STAR Collaboration), Phys. Rev. Lett. **92**, 052302 (2004).
 - [2] D. Teaney, Phys. Rev. C **68**, 034913 (2003).
 - [3] P. Huovinen *et al.*, Phys. Lett. B **503**, 58 (2001).
 - [4] L. P. Csernai, J. I. Kapusta, and L. D. McLerran, Phys. Rev. Lett. **97**, 152303 (2006); R. Lacey *et al.*, Phys. Rev. Lett. **98**, 092301 (2007).
 - [5] G. Policastro, D. T. Son and A. O. Starinets, Phys. Rev. Lett. **87**, 081601 (2001); P. K. Kovtun, D. T. Son and A. O. Starinets, Phys. Rev. Lett. **94**, 111601 (2005).
 - [6] T. Hirano and K. Tsuda, Phys. Rev. C **66**, 054905 (2002).
 - [7] P. Romatschke and U. Romatschke, Phys. Rev. Lett. **99**, 172301 (2007).
 - [8] M. Bleicher and H. Stöcker, Phys. Lett. B **526**, 309 (2002).
 - [9] D. Molnar and M. Gyulassy, Nucl. Phys. **A697**, 495 (2002); **A703**, 893(E) (2002).
 - [10] Z. Xu and C. Greiner, Phys. Rev. C **71**, 064901 (2005).
 - [11] Z. Xu and C. Greiner, Phys. Rev. C **76**, 024911 (2007).
 - [12] S. Mrówczyński, Phys. Lett. B **314**, 118 (1993); Phys. Rev. C **49**, 2191(1994); P. Arnold, J. Lenaghan, and G.D. Moore, J. High Energy Phys. **08** (2003) 002; P. Arnold *et al.*, Phys. Rev. Lett. **94**, 072302 (2005); A. Rebhan, P. Romatschke, and M. Strickland, Phys. Rev. Lett. **94**, 102303 (2005); A. Dumitru and Y. Nara, Phys. Lett. B **621**, 89 (2005).
 - [13] Z. Xu and C. Greiner, Phys. Rev. Lett. **100**, 172301 (2008).
 - [14] A. Adil *et al.*, Phys. Rev. C **74**, 044905 (2006); H. J. Drescher *et al.*, Phys. Rev. C **76**, 024905 (2007).
 - [15] T.S. Biro *et al.*, Phys. Rev. C **48**, 1275 (1993); S.M.H. Wong, Nucl. Phys. **A607**, 442 (1996).
 - [16] B. B. Back *et al.* (PHOBOS Collaboration), Phys. Lett. B **578**, 297 (2004).
 - [17] I. G. Bearden *et al.* (BRAHMS Collaboration), Phys. Rev. Lett. **94**, 162301 (2005); I. Arsene *et al.* (BRAHMS Collaboration), Nucl. Phys. **A757**, 1 (2005).
 - [18] J. Adams *et al.* (STAR Collaboration), Phys. Rev. C **72**, 014904 (2005); B. B. Back *et al.* (PHOBOS Collaboration), Phys. Rev. C **72**, 051901(R) (2005).
 - [19] D. Molnar and S. A. Voloshin, Phys. Rev. Lett. **91**, 092301 (2003); P. F. Kolb *et al.*, Phys. Rev. C **69**, 051901(R) (2004).
 - [20] X. Zhu, M. Bleicher, and H. Stöcker, Phys. Rev. C **72**, 064911 (2005); L. W. Chen *et al.*, Phys. Lett. B **605**, 95 (2005); T. Hirano *et al.*, Phys. Lett. B **636**, 299 (2006); J. Bleibel *et al.*, Phys. Rev. C **76**, 024912 (2007).